nature climate change

ARTICLES

https://doi.org/10.1038/s41558-020-0883-0

Current and future global climate impacts resulting from COVID-19

Piers M. Forster[1]✉, Harriet I. Forster[2], Mat J. Evans[3,4], Matthew J. Gidden[5,6], Chris D. Jones[7], Christoph A. Keller[8,9], Robin D. Lamboll[10], Corinne Le Quéré[11,12], Joeri Rogelj[6,10], Deborah Rosen[1], Carl-Friedrich Schleussner[5,13], Thomas B. Richardson[1], Christopher J. Smith[1,6] and Steven T. Turnock[1,7]

The global response to the COVID-19 pandemic has led to a sudden reduction of both GHG emissions and air pollutants. Here, using national mobility data, we estimate global emission reductions for ten species during the period February to June 2020. We estimate that global NO_x emissions declined by as much as 30% in April, contributing a short-term cooling since the start of the year. This cooling trend is offset by ~20% reduction in global SO_2 emissions that weakens the aerosol cooling effect, causing short-term warming. As a result, we estimate that the direct effect of the pandemic-driven response will be negligible, with a cooling of around 0.01 ± 0.005 °C by 2030 compared to a baseline scenario that follows current national policies. In contrast, with an economic recovery tilted towards green stimulus and reductions in fossil fuel investments, it is possible to avoid future warming of 0.3 °C by 2050.

By the time the World Health Organization declared COVID-19 (scientifically referred to as the severe acute respiratory syndrome–coronavirus 2 or SARS-CoV-2) a pandemic on 11 March 2020, the virus had already spread from China to other Asian countries, Europe and the United States. As of 5 July 2020, cases have been identified in 188 countries or regions[1]. This has led to unprecedented enforced and voluntary restrictions on travel and work. This in turn has led to reductions of both GHG emissions and air pollutants[2–4]. Analysis of mobility data from Google[5] and Apple[6] shows that mobility declined by 10% or more during April 2020 in all but one of the 125 nations tracked. Mobility declined by 80% in five or more nations (Supplementary Fig. 1). Associated declines in air pollution have been observed from satellite data and from local ground-based observations[7,8]. The large pollution declines are expected to be temporary as pollution levels are already returning to near-normal in parts of Asia[9,10].

Here we build an estimate of emission changes in GHGs and air pollution due to the COVID-19 global restrictions during the period February–June 2020 and project these into the future. These emission changes are then used to make a prediction of the resultant global temperature response. We examine the temperature response of a direct recovery to pre-COVID-19 national policies and emission levels, and also explore responses where the economic recovery to COVID-19 is driven by either a green stimulus package or an increase in fossil fuel use.

Emission trends

Bottom-up emission-trend analyses have traditionally relied on laborious collection of various energy-industry-related indicators and statistics from multiple sources[11]. The unprecedented recent access to global mobility data from Google and Apple gives a unique opportunity to compare trends across many countries with a consistent approach. We use these data to develop a new method of emission-trend analysis. The advantage over previous approaches is the possibility of near-real-time analysis, national granularity and a systematic consistent approach across nations and over time. The disadvantages are the loss of a direct connection between energy and emissions and the need to make assumptions about these relationships. There are also disadvantages over the short time history of the mobility data and opacity from the data providers around their detailed methodologies and uncertainties. Here we make a simple set of assumptions to deduce estimates of emissions change from the mobility data and test the estimates extensively against the approach of Le Quéré et al.[3].

Google and Apple mobility changes and the Le Quéré et al.[3] data all indicate that >50% of the world's population reduced travel by >50% during April 2020 (Fig. 1a). Google mobility trends indicate that >80% of the population in the 114 countries in the dataset (4 billion people) reduced their travel by >50%. Google mobility data and emission reduction estimates based on confinement level analysis in Le Quéré et al.[3] agree on country-level surface-transport trends to within ~20% (Fig. 1b and Supplementary Fig. 1). When we examine the trends for the countries that we expect have contributed most to the overall surface-transport emission change (for example, the United States, European nations and India), good agreement between the datasets is observed and their trends are well-correlated in time (see Fig. 1b and Extended Data Fig. 1). Workplace, retail and residential movement data from Google also compare relatively well

[1]Priestley International Centre for Climate, University of Leeds, Leeds, UK. [2]Queen Margaret's School, Escrick, York, UK. [3]Wolfson Atmospheric Chemistry Laboratories, Department of Chemistry, University of York, York, UK. [4]National Centre for Atmospheric Science, University of York, York, UK. [5]Climate Analytics, Berlin, Germany. [6]Energy Program, International Institute for Applied Systems Analysis, Laxenburg, Austria. [7]Met Office Hadley Centre, Exeter, UK. [8]NASA Global Modeling and Assimilation Office, Goddard Space Flight Center, Greenbelt, MD, USA. [9]Universities Space Research Association, Columbia, MD, USA. [10]Grantham Institute for Climate Change and the Environment, Imperial College London, London, UK. [11]School of Environmental Sciences, University of East Anglia, Norwich, UK. [12]Tyndall Centre for Climate Change Research, University of East Anglia, Norwich, UK. [13]IRI THESys, Humboldt University, Berlin, Germany. ✉e-mail: p.m.forster@leeds.ac.uk

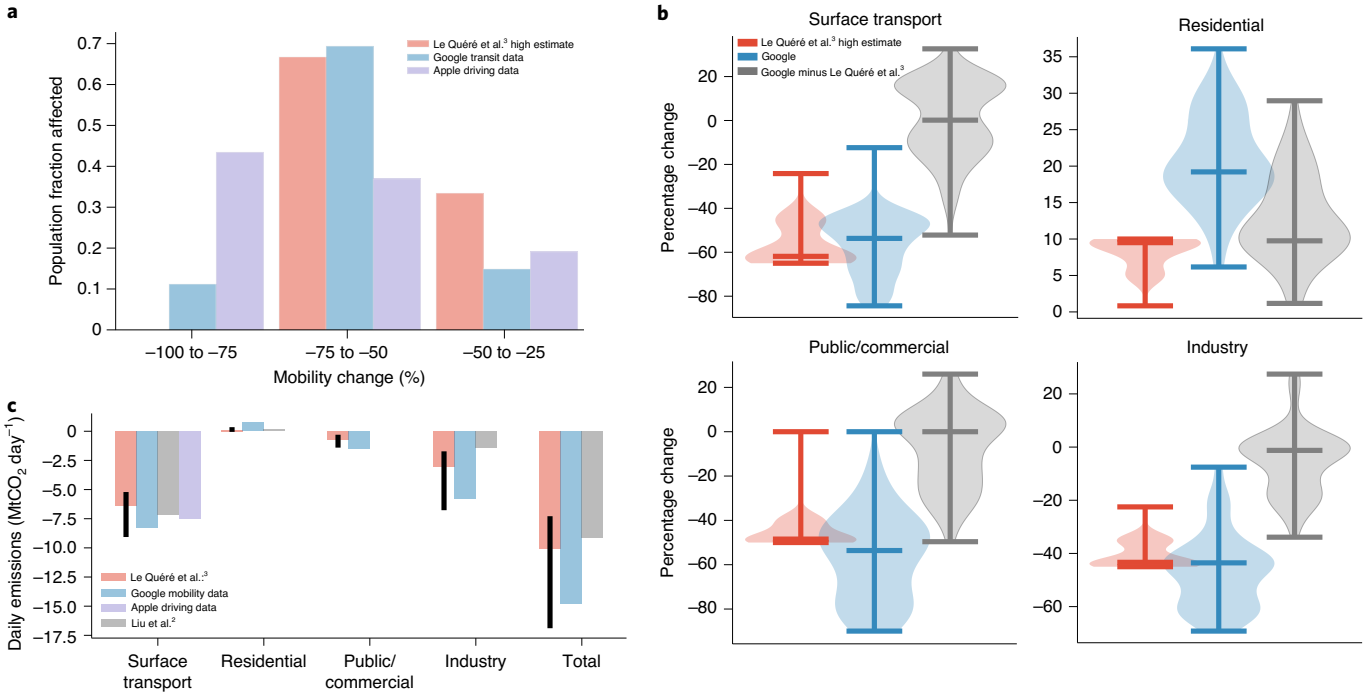

Fig. 1 | Comparison of sector emission trends. a, Population-weighted histogram of surface-transport trends from Apple driving data, Google transit mobility data and the high estimate from Le Quéré et al.[3] for available countries in the different datasets averaged over April 2020. **b**, Violin plots showing the distribution, minimum, maximum and median levels of national trends weighted by CO_2 emissions for the Google and Le Quéré et al.[3] datasets and the differences between the datasets evaluated over April 2020. **c**, Estimates of emission changes for the datasets across four sectors for April 2020 and the sum of the four sectors. The CO_2 emission estimates from Liu et al.[2] are also shown on this panel. In **b** and **c**, data are shown for 60 countries with overlapping data in the Google and Le Quéré et al.[3] datasets (representing 60% of global CO_2 emissions). In **c**, Apple data are shown for 57 countries, covering 58% of the global emissions. The Liu et al.[2] estimate is for a global emission change. The high estimate from Le Quéré et al.[3] data is used in **a** and **b**. Panel **c** shows the Le Quéré et al.[3] low and high estimates as the range of the error bar on the mid-level estimate. For baselines, see Methods.

with corresponding industry, public and residential sector emission changes but only if the high estimate of the emission change in the Le Quéré et al.[3] dataset (Fig. 1b,c and Supplementary Figs. 3 and 4) is used.

Using mobility data outside of the surface-transport sector is likely to overestimate the emission change and this appears to be the case for CO_2 emissions when compared to two previous estimates[1,2]. Nevertheless, our national and US state-level mobility-derived emission estimates are well-correlated in time with emission changes from the Le Quéré et al.[3] study (see examples in Supplementary Figs. 3 and 4). For the industry sector, differences may be due to the fact that the emissions from industrial activity are less correlated with mobility trends, due to automated machinery, inertia in closing operations or alternative modes of work, or a baseline level of industrial emission from heavy industry in the absence of production, neither which would be captured by the Google mobility data which only report changes in phone locations. For the residential sector, the 20% median increase matches the UK smart meter analysis by Octopus Energy for the situation when previously empty houses were occupied during the day after lockdown restrictions began[12]. However, many households were already occupied during the day and in these situations, when an additional occupant was added, energy use only increased by 4%. These factors probably mean that our Google-based trends overestimate the emission change from these sectors, leading to our Google-based total emission-trend estimate agreeing better with the high emission estimate from the Le Quéré et al.[3] dataset. Our analysis also suggests considerably larger trends than those found in Liu et al.[2] (compare datasets in Fig. 1c). There is also a question about how representative the Apple and Google datasets are of wider national behaviour and how the use and penetration of these phone operating systems varies across regions[13]. For example, the >80% drop in Apple driving mobility in India (Fig. 1a and Supplementary Fig. 1), may only represent the part of the population that are able to work from home. Therefore, the emissions trends in our work which are largely derived from Google mobility data should be taken as a high estimate of the COVID-19 emission-driven change (see Methods).

In the following, we construct 2020 emission changes largely from Google mobility data to estimate emissions changes from the restriction measures in response to the COVID-19 virus, as illustrated in Fig. 1c. As Google data are not available everywhere, we use the Le Quéré et al.[3] analysis to cover important missing countries, in particular, China and Iran, which are large emitters whose citizens have been under considerable restrictions related to COVID-19. We also use Le Quéré et al.[3] data to provide additional trend estimates from aviation and shipping sectors (see Methods).

Our bottom-up analysis uses 123 countries covering >99% of global fossil fuel CO_2 emissions, extending the 69 countries analysed in Le Quéré et al.[3]. Daily national emission trends in six sectors are analysed for January–June 2020 (surface transport, residential, power, industry, public and aviation). These are then weighted by the national and sector split of seven emitted species covering the major GHGs and short-lived pollutants. The estimated changes in these non-CO_2 species covers their total anthropogenic emissions, although agricultural and waste emissions are assumed not to change (Methods). National and sector data are taken from the Emissions Database for Global Atmospheric Research (EDGAR) v.5.0 database for 2015[14]. These data are combined to generate

Table 1 | Pathway 'what-if' assumptions

Pathway	What happens	Notes
Baseline	Follows emissions until 2030, consistent with a successful implementation of the current NDC submitted by individual countries under the Paris Agreement, adapted from Rogelj et al.[15]. Emissions continue after 2030, assuming no significant strengthening in climate action.	The data are adapted from Rogelj et al.[15] and represents a central estimate of the range of estimates presented therein. This pathway also falls centrally in the range identified by the 2019 UNEP Emissions Gap Report[30].
Two-year blip	Reflecting potential SARS-CoV-2 transmission dynamics[22], this case explores 66% of the June 2020 lockdown persisting until the end of 2021, then emissions linearly recover to baseline by the end of 2022.	This implies a persistent necessity of partial lockdowns until the end of 2023 but with no lasting effect of SARS-CoV-2.
Fossil-fuelled recovery	Follows the two-year blip pathway until the end of 2021, then emissions recover in a way similar to the recovery after the 2008/9 global recession, rebounding to 4.5% above the baseline at the end of 2022. Stimulus packages are designed with strong support for fossil-fuel energy supply, resulting in more fossil investment than a pre-COVID-19 current-policy scenario (+1%) and considerably less in low-carbon alternatives (−0.8%). Resulting emissions are 10% higher in 2030 than the baseline scenario, a trend that is assumed to continue thereafter[31].	2030 data taken from Climate Action Tracker[31], 'rebound to fossil-fuel scenario' with the relative increase in emissions compared to baseline continued thereafter.
Moderate green stimulus	Follows the two-year blip pathway until end of 2021, then emissions recover slightly, until the end of 2022 but never reach the baseline projections. Governments choose recovery packages to target specifically low-carbon energy supply and energy efficiency, and do not support bailouts for fossil firms. The resulting investment differential (+0.8% for low-carbon technologies and −0.3% for fossil fuels relative to a current-policy scenario) begins to structurally change the emissions intensity of economic activity, resulting in about a 35% decrease in GHG emissions by 2030 relative to the baseline scenario, a trend that is assumed to continue thereafter[31], consistent with meeting global net-zero CO_2 by 2060.	Short-term benefits come from changes to the norms of behaviour, then green incentives to decarbonize all sectors of the economy.
Strong green stimulus	As for the moderate green stimulus with investment differentials (+1.2% for low-carbon technologies and −0.4% for fossil fuels relative to a current-policy scenario), resulting in a slightly more than 50% decrease of GHG emissions by 2030 relative to the baseline scenario. This trend is continued thereafter, consistent with meeting global net-zero CO_2 by 2050.	This has >50% chance of limiting the 2050 temperature rise to 1.5 °C above pre-industrial.

national and globally averaged daily emission changes in 2020 by species and sector.

To assess changes due to the COVID-19 pandemic, we establish a baseline scenario. We take a central estimate of emissions pathways[15], in which countries are assumed to meet their stated nationally determined contributions (NDCs) by 2030. In this baseline, no further strengthening of climate action after 2030 is assumed to take place. These pathways account for both GHG and air pollutant emission changes (see Methods). To derive changes from this scenario, a three-stage process is followed (see Methods). First, fractional Google mobility data use the five-week period (3 January to 6 February 2020) as reference. Absolute emission trends are then computed by multiplying these fractional changes by either the 2019 CO_2 emissions from Le Quéré et al.[3] or, for other species, the 2015 emissions in the EDGAR database[14]. Finally, these absolute changes are then applied to a steadily rising emission pathway based on pre-COVID-19 national pledges (see Table 1). Only the globally average emission changes are used in this paper (see Fig. 2a) but national and spatially gridded data are made available for other interested researchers (https://doi.org/10.5281/zenodo.3957826).

Our analysis shows that emission reductions probably peaked in mid-April 2020 and that these reductions are species dependent. The data suggest that global fossil fuel CO_2 emissions and total NO_x emissions could have decreased by as much as 30% in April 2020 driven by a decline in surface-transport emissions (Fig. 2a,b and Supplementary Fig. 5). Conversely, organic carbon (OC) has increased by <1% as it is primarily affected by rising residential emissions (Fig. 2b and Supplementary Fig. 5). Methane changes are driven by power sector declines and SO_2 is most strongly affected by declining industrial emissions. Generally, changes in surface transport are the biggest driver of change for most species analysed (Supplementary Fig. 5). The analysis in Fig. 2b also applies our methods to the Le Quéré et al.[3] data for non-CO_2 species and reports both previous estimates of CO_2 trend. Our estimated trends are close to the high Le Quéré et al. estimate and almost twice as large as the CO_2 trend estimate of Liu et al.[2].

Our data suggest that changes in emissions are not confined to the major emitting countries and mobility restrictions have been of worldwide proportions (despite the extent of measures—and therefore relative emissions changes—varying globally) during April 2020 (Fig. 1 and Supplementary Fig. 1). This manifests itself in many countries contributing to the emission decline. For the short-lived species, Europe and the United States, in spite of their large fractional national emission change, make up a small percentage of the global response due their relatively low levels of emissions from pollution (Fig. 2b and Supplementary Fig. 6).

Observational evidence

Detecting a COVID-19-related signal in CO_2 concentrations is challenging due to the long atmospheric lifetime of CO_2 which makes any perturbation small. While the airborne fraction of CO_2 emissions is ~50% on multi-annual timescales[11], the airborne fraction of emissions changes is probably above 90% on subannual timescales[16]. Because CO_2 is not well mixed on the timescale of weeks to months, individual observing stations will not reflect the global CO_2 burden—for example, Mauna Loa in the Northern hemisphere Pacific Ocean may see a larger signal than at the South Pole from the emissions reductions due to COVID-19 restrictions. The magnitude of natural (terrestrial and marine) fluxes of CO_2 compared

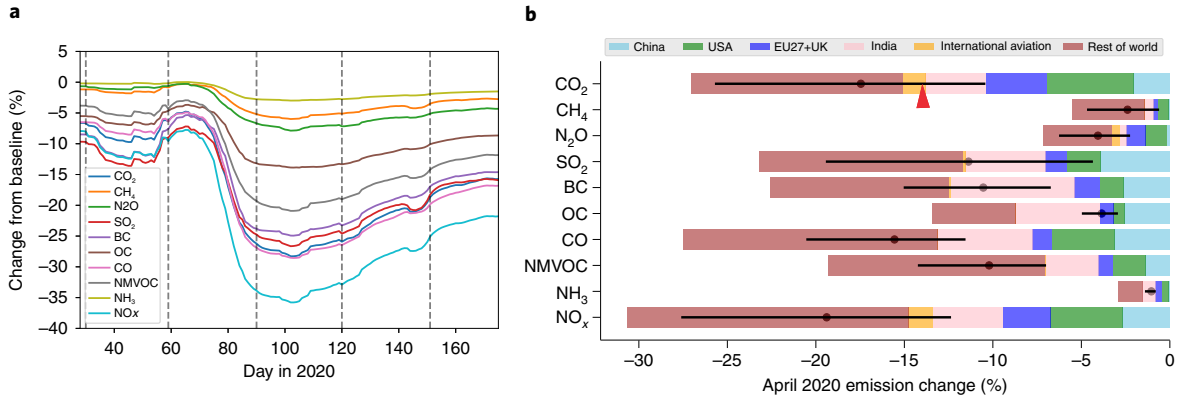

Fig. 2 | Species-derived changes from COVID-19 restrictions. a, Percentage globally averaged emission changes for the considered species as a function of day in the year of 2020. The changes are for fossil fuel CO_2 emissions and total anthropogenic emissions from the other sectors. The vertical grey dashed lines mark the first day of the months Febuary to June to aid orientation. **b**, A breakdown of the April 2020 average global emission reductions compared to a recent year for the different species. The breakdown is for major emission-producing nations, including international aviation. Global percentage emission changes from the baseline are shown on the *x* axis (see details in Supplementary Figs. 5 and 6). Trends are relative to 2019 for CO_2; for the other species they are relative to 2015. The low, middle and high estimates of the total changes based on Le Quéré et al.[3] and Liu et al.[2] trends are shown for comparison as the black circles, error bars and red triangle. EU27+UK, the 27 countries in the European Union plus the United Kingdom.

with anthropogenic emissions make it extremely difficult to detect changes in emissions at national level from CO_2 concentrations themselves. We estimate these CO_2 concentration changes in the temperature response to restrictions section (see Fig. 5b) and find maximum reductions compared to our baseline scenario of around 2 ppm in two years' time (Extended Data Fig. 2).

Even though the CO_2 change cannot readily be observed, changes in the concentrations of air pollutants can be used to test the veracity of the bottom-up emission reduction estimates. A decline in NO_2 has been observed globally and in several countries and cities[7,8]. NO_2 is short-lived (~5 h), provides a relatively linear response to emission changes (unlike other pollutants, such as O_3 and PM2.5) and reductions in its emissions are expected to be well-correlated to CO_2 emission reductions (see Fig. 2a and Le Quéré et al.[3]). Changes in its concentration thus act as a useful bellwether for changes in CO_2 emissions. A number of studies report COVID-19-induced changes in NO_2 concentration from both surface- and satellite-platforms over China[17,18]. However, it remains challenging to get a quantifiable estimate of the emission-driven NO_2 change as it is hard to separate that signal from meteorological variability. To address this we follow previous work[19] and develop a machine-learning method to derive meteorology and chemistry-normalized changes in NO_2 surface concentrations at air quality monitoring stations around the globe (see Methods). We aggregate these changes for 32 nations and show how these observationally based national time series of NO_2 concentration changes compare to our mobility-based estimate of NO_x emissions change in Supplementary Fig. 7. Figure 3 shows the predicted mobility-based NO_x emissions change versus the average observationally derived NO_2 change for each country in 2020. Some differences between the emission estimates and observed changes would be expected: monitoring stations tend to focus on sites with high surface-transport emission and so may be less sensitive to changes in industrial or residential activity; much of the surface-transport emissions of NO_x arises from commercial vehicles (64% of surface-transport emission in the United Kingdom[20]) which may show different responses to the population aggregated mobility data used here (see Methods and Supplementary Fig. 2). However, the comparisons for the individual countries (Supplementary Fig. 7) are generally good and there is a quantitative relationship between the average predicted change in the emissions and observed reduction in concentrations (Fig. 3). Most countries show a smaller (20% or roughly two percentage points) decrease in observed NO_2 than the predicted reduction in NO_x emissions, whereas China and India show larger observed reductions than predicted (28% and 48%, respectively). This could be due to the Le Quéré et al.[3] analysis being used to estimate trends in China as Google data were not available and also due a possible lack of representativeness in the phone mobility data for India (see Emission trends). As China is the largest emitter, our analyses might be affected by a possible significant underestimate of Chinese NO_x trends and hence global trend in the early part of the record, although any global underestimate is unlikely to have persisted into April, where the contribution of China to the global trend is relatively modest (Fig. 2b).

The temperature response to restrictions

The immediate response of the warming comes from a combination of an aerosol-induced warming trend and a cooling trend both from CO_2 reductions and the NO_x-driven tropospheric ozone cooling loss (Fig. 4). To estimate the surface temperature response beyond April 2020, the emission trends are projected forward in time under four simple 'what-if' assumptions. The temperature changes from these pathways were simulated by the FaIR v1.5 climate emulator[21] which was set up to represent the response expected from the latest generation of climate models (see Methods). As significant social distancing conditions may be necessary for two years[22], we begin by assuming in all pathways that the emissions decrease will remain at 66% of their June 2020 values until the end of 2021. In the simplest 'two-year blip' pathway, emissions return linearly to the baseline pathway by the end of 2022 (Table 1 and Fig. 4a). Under such a pathway, we project a longer term cooling from reductions in CO_2 of around 0.01 ± 0.005 °C compared to baseline, with a cancellation of the influence of the removal of short-term pollutants (Fig. 4b and Extended Data Fig. 2).

As the global temperature response due to COVID-19 restrictions will probably be small, climate scientists are encouraged to look for regional climate signatures. In particular, changes in aerosol loadings may contribute to increasing regional risks posed by extreme weather, such as heat waves or heavy precipitation[23,24]. Such near-term changes require particular attention as hazards posed by extreme weather will compound with the ongoing pandemic situation, as exemplified tragically by tropical cyclone Amphan hitting Kolkata on 21 May 2020. With considerable overlaps of

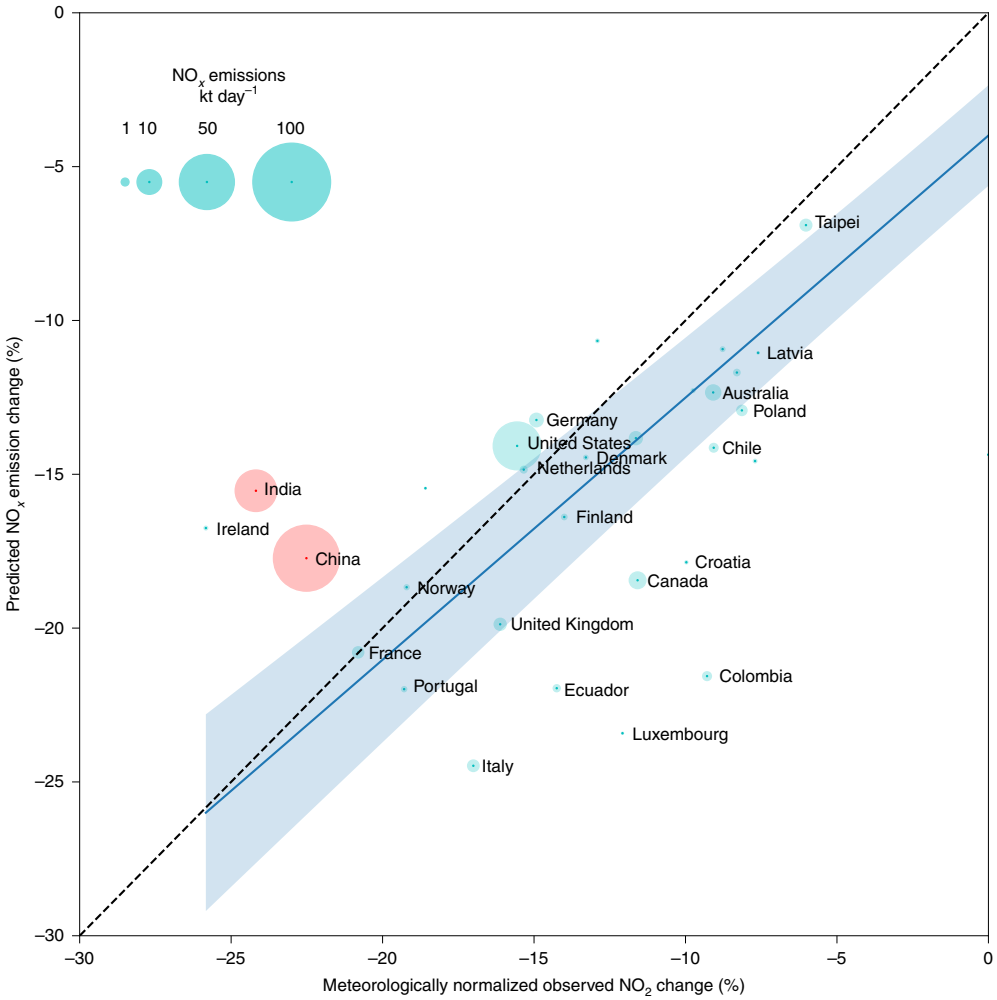

Fig. 3 | Comparison with observations. Country-level comparison of the mean predicted NO_x emissions change against the meteorologically normalized observed mean fractional reduction in NO_2 concentration for the period 1 January to 11 May 2020. Circle size indicates the mass of NO_x emitted each day for that country from EDGAR emissions. The blue line shows the line of best fit (orthogonal regression) excluding China and India shown in red, weighted by the number of observations in those countries, with the shaded area showing the 95% confidence interval. Not all countries are labelled. Brazil shows an increase in NO_2 concentrations and is not shown but is included in the statistical fit (see also Supplementary Fig. 7).

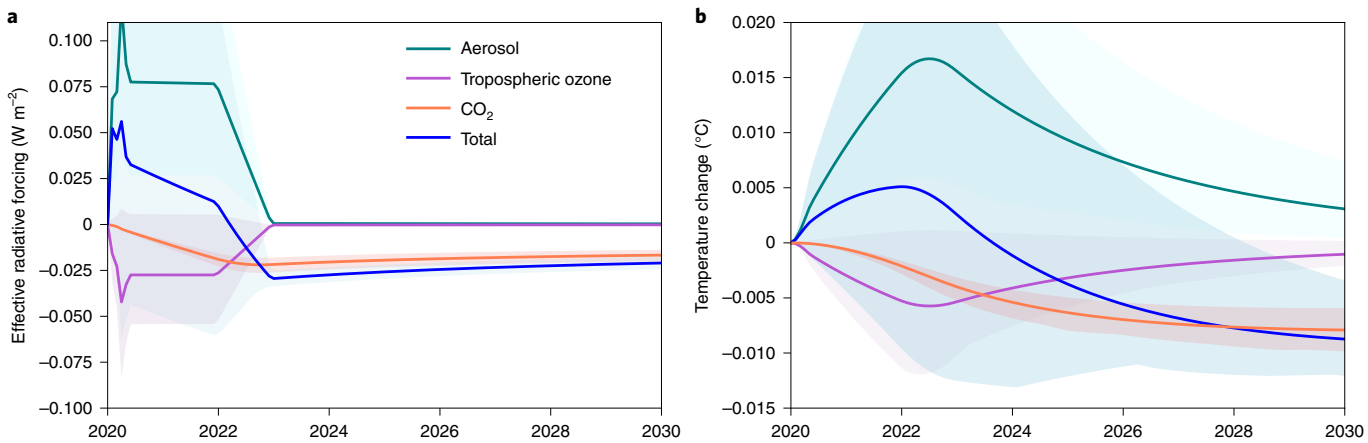

Fig. 4 | Response to the two-year blip pathway. a,**b**, Component effective radiative forcing (**a**) and component temperature response (**b**). Results are for the two-year blip pathway compared to the baseline pathway. The response is broken down by the major forcing contributors, as emulated by the FaIR v.1.5 model. The 5–95% Monte Carlo sampled uncertainties are shown and weighted according to their historical fit to the surface temperature record (see Methods).

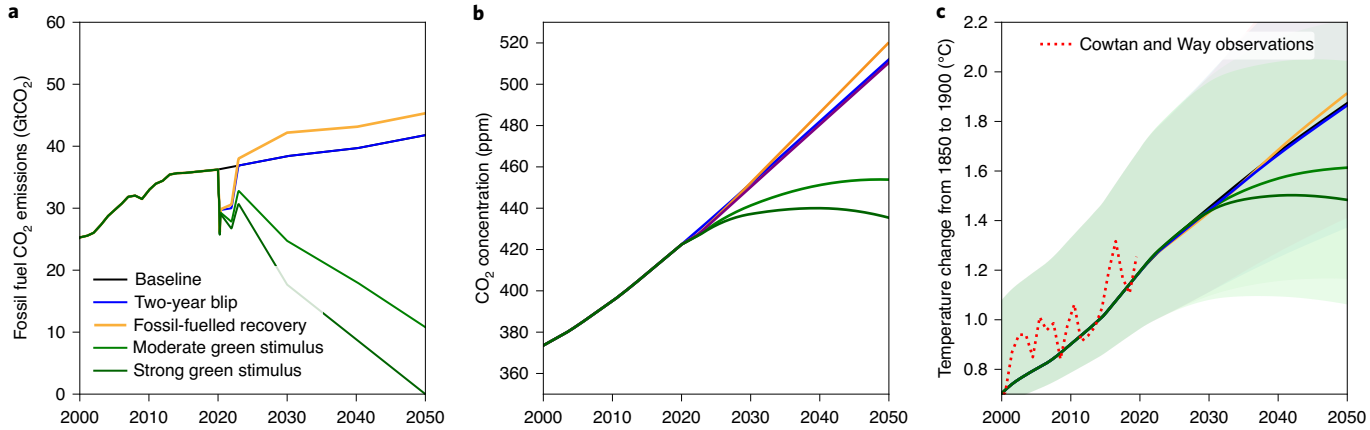

Fig. 5 | Longer term climate response. a–c, Emissions of CO_2 (**a**), CO_2 concentrations (**b**) and the global surface air temperature response (**c**) for the what-if pathways from Table 1, emulated by the FaIR v.1.5 model. The baseline pathway is also plotted but largely obscured by the two-year-blip pathway. The 5–95% Monte Carlo sampled uncertainties are shown and weighted according to their historical fit to observations (red dotted line)[32] shown in **c** (see Methods).

vulnerable groups (for example, heat waves and the elderly) or challenges related to the implementation of effective responses (evacuation in case of flooding), as well as potential impacts on crop yields[25] and initial studies suggesting that the spread of COVID-19 may itself be influenced by climatic factors[22], this will put the ability of society and governments to manage compound risks to the test[26].

In our estimates, declines in NO_x of as much as 30% will contribute a short-term cooling of up to 0.01 °C over the period 2020–2025 almost exclusively from reductions in tropospheric ozone. NO_x trends also contribute an insignificant warming effect from the decrease in nitrate aerosol. As the ozone response is expected to have strong regional variation, we test the ozone response in a more sophisticated emulator[27,28] that takes these variations into account (see Methods). This estimates an annual mean radiative forcing of $-0.029\,W\,m^{-2}$ for 2020, in very close agreement with the forcing seen in Fig. 4a ($-0.030\,W\,m^{-2}$). The emulator also provides an estimate of the regional mean surface ozone changes (Supplementary Table 4). In contrast to NO_x, reductions in emissions of other short-lived pollutants, especially SO_2, cause warming from weakening negative aerosol forcing. These two effects more-or-less cancel in our simulations, although on balance we expect a small warming effect over the next two years (Fig. 4b).

In spite of the uncertainty, our results indicate that reductions of NO_x have a cooling effect which will probably offset a considerable fraction of the warming that comes from reductions in emissions of other short-lived pollutants. This suggests that policies directed at limiting pollution from road transport could offset the short-term warming that might come from policies that reduce pollution from the power and industry sector. Therefore, we recommend that policies are enacted to cut pollution from all three sectors at the same time. This is a useful way forward for net-zero transition pathways so we can avoid any short-term warming effects that might come from reductions in aerosol pollution[29].

The need for a green recovery

As we have shown, the climate effect of the immediate COVID-19-related restrictions is close to negligible and lasting effects, if any, will only arise from the recovery strategy adopted in the medium term. To that end, we assess the effect of different scenarios including a fossil-fuelled recovery and two different scenarios of green stimulus (all pathway assumptions are summarized in Table 1).

Due to the different warming and cooling trends from short-lived pollutants, the 2020–2030 climate response to the different pathways remains uncertain but is probably negligible whatever path the recovery takes (Figs. 4 and 5 and Extended Data Figs. 3 and 4). However, differences manifest themselves after 2030. Figure 5 shows estimated changes in CO_2 emissions and the climatic responses for the four assessed pathways. We find that both the two-year blip pathway, where the economic recovery maintains current investment levels, and the fossil-fuelled recovery pathway are likely to exceed 1.5 °C above pre-industrial limit by 2050 (>80%; Extended Data Fig. 5). Conversely, choosing a pathway with strong green stimulus assumptions (~1.2% of global gross domestic product), including climate policy measures, has a good chance (~55%; Extended Data Fig. 5) of keeping global temperature change above pre-industrial within the 1.5 °C limit, saving around 0.3 °C of future warming by 2050 (0.2 °C for the moderate green stimulus pathway).

Our work shows that the global temperature signal due to the short-term dynamics of the pandemic is likely to be small. These results highlight that without underlying long-term system-wide decarbonization of economies, even massive shifts in behaviour, only lead to modest reductions in the rate of warming. However, economic investment choices for the recovery will strongly affect the warming trajectory by mid-century. Pursuing a green stimulus recovery out of the post-COVID-19 economic crisis can set the world on track for keeping the long-term temperature goal of the Paris Agreement within sight.

Lastly, by combining large datasets from surface air quality networks with mobility data, we have illustrated the science benefits from timely and easy access to big data. Such data syntheses can help epidemiology and environmental sciences to provide the evidence base for the solutions that are urgently needed to build a resilient recovery to the devastating pandemic. Google, Apple and other big data providers are encouraged to continue to provide and expand their data offerings.

Online content

Any methods, additional references, Nature Research reporting summaries, source data, extended data, supplementary information, acknowledgements, peer review information; details of author contributions and competing interests; and statements of data and code availability are available at https://doi.org/10.1038/s41558-020-0883-0.

Received: 1 June 2020; Accepted: 24 July 2020;
Published online: 7 August 2020

References

1. *COVID-19 Map* (Johns Hopkins Coronavirus Resource Center, accessed 5 July 2020); https://coronavirus.jhu.edu/map.html
2. Liu, Z. et al. COVID-19 causes record decline in global CO_2 emissions. Preprint at http://arxiv.org/abs/2004.13614 (2020).
3. Le Quéré, C. et al. Temporary reduction in daily global CO_2 emissions during the COVID-19 forced confinement. *Nat. Clim. Change* **10**, 647–653 (2020).
4. *COVID-19 Air Quality Worldwide Dataset* (The World Air Quality Project, accessed 5 July 2020); https://aqicn.org/data-platform/covid19/
5. *Google LLC Community Mobility Reports* (Google, accessed 5 July 2020); https://www.google.com/covid19/mobility/
6. *Apple LLC Mobility Trends Reports* (Apple, accessed 5 July 2020); https://www.apple.com/covid19/mobility
7. Bauwens, M. et al. Impact of coronavirus outbreak on NO_2 pollution assessed using TROPOMI and OMI observations. *Geophys. Res. Lett.* **47**, e2020GL087978 (2020).
8. Shi, X. & Brasseur, G. P. The response in air quality to the reduction of Chinese economic activities during the COVID-19 outbreak. *Geophys. Res. Lett.* **47**, e2020GL088070 (2020).
9. *China's Air Pollution Overshoots Pre-crisis Levels for the First Time* (CREA, accessed 24 May 2020); https://energyandcleanair.org/china-air-pollution-rebound-briefing/
10. Zhang, R. et al. NOx emission reduction and recovery during COVID-19 in East China. *Atmosphere* **11**, 433 (2020).
11. Friedlingstein, P. et al. Global carbon budget 2019. *Earth Syst. Sci. Data* **11**, 1783–1838 (2019).
12. *Domestic Energy Usage Patterns During Social Distancing* (Octopus Energy, accessed 24 May 2020); https://octopus.energy/blog/domestic-energy-usage-patterns-during-social-distancing/
13. *Operating System Market Share Worldwide* (StatCounter Global Stats, accessed 24 May 2020); https://gs.statcounter.com/os-market-share#quarterly-201903-201903-map
14. Crippa, M. et al. High resolution temporal profiles in the emissions database for global atmospheric research. *Sci. Data* **7**, 1–17 (2020).
15. Rogelj, J. et al. Understanding the origin of Paris Agreement emission uncertainties. *Nat. Commun.* **8**, 1–12 (2017).
16. Jones, C. D. et al. Simulating the earth system response to negative emissions. *Environ. Res. Lett.* **11**, 95012 (2016).
17. Le, T. et al. Unexpected air pollution with marked emission reductions during the COVID-19 outbreak in China. *Science* https://doi.org/10.1126/science.abb7431 (2020).
18. Liu, F. et al. Abrupt decline in tropospheric nitrogen dioxide over China after the outbreak of COVID-19. *Sci. Adv.* https://doi.org/10.1126/sciadv.abc2992 (2020).
19. Grange, S. K. & Carslaw, D. C. Using meteorological normalisation to detect interventions in air quality time series. *Sci. Total Environ.* **653**, 578–588 (2019).
20. Richmond, B. et al. *UK Informative Inventory Report (1990 to 2018)* (BEIS, 2020).
21. Smith, C. J. et al. FAIR v1.3: a simple emissions-based impulse response and carbon cycle model. *Geosci. Model Dev.* **11**, 2273–2297 (2018).
22. Kissler, S. M., Tedijanto, C., Goldstein, E., Grad, Y. H. & Lipsitch, M. Projecting the transmission dynamics of SARS-CoV-2 through the postpandemic period. *Science* **368**, 860–868 (2020).
23. Luo, F. et al. Projected near-term changes of temperature extremes in Europe and China under different aerosol emissions. *Environ. Res. Lett.* **15**, 034013 (2020).
24. Samset, B. H. et al. Climate impacts from a removal of anthropogenic aerosol emissions. *Geophys. Res. Lett.* **45**, 1020–1029 (2018).
25. Dentener, F. et al. Lower air pollution during COVID-19 lock-down: improving models and methods estimating ozone impacts on crops. Preprint at https://eartharxiv.org/de9fs/ (2020).
26. Phillips, C. A. et al. Compound climate risks in the COVID-19 pandemic. *Nat. Clim. Change* **10**, 586–588 (2020).
27. Turnock, S. T. et al. The impact of future emission policies on tropospheric ozone using a parameterised approach. *Atmos. Chem. Phys.* **18**, 8953–8978 (2018).
28. Turnock, S. T., Wild, O., Sellar, A. & O'Connor, F. M. 300 years of tropospheric ozone changes using CMIP6 scenarios with a parameterised approach. *Atmos. Environ.* **213**, 686–698 (2019).
29. Shindell, D. & Smith, C. J. Climate and air-quality benefits of a realistic phase-out of fossil fuels. *Nature* **573**, 408–411 (2019).
30. *Emissions Gap Report 2019* (UNEP, 2020).
31. *Climate Action Tracker Update: A Government Roadmap for Addressing the Climate and Post COVID-19 Economic Crises Summary and Conclusions* (Climate Action Tracker, 2020).
32. Cowtan, K. & Way, R. G. Coverage bias in the HadCRUT4 temperature series and its impact on recent temperature trends. *Q. J. R. Meteorol. Soc.* **140**, 1935–1944 (2014).

Methods

CO_2 emission estimates. *The Google mobility analysis.* Google[5] and Apple[6] mobility data were accessed on 5 July 2020. National average Google data were used for 114 countries and the US states. Mobility was provided in six categories of which we used four in our analyses (transit stations, residential, workplaces and retail and recreation). These data represent the number of Android phones at assigned locations, representing transit stations, homes, workplaces, retail outlets and parks. Apple mobility data were from phone movement changes available for 57 countries providing data on changes in transit use, walking and driving, depending on country. Google data were referenced to the day-of-week average in the five-week period from 3 January to 6 February 2020. Apple used a baseline of 13 February and did not account for day-of-week effects. The Apple data were considerably more variable and were only used as a check on the other datasets. Our tests found that the Google transit mobility trends agreed well with Apple driving trends in the 56 nations with overlapping data (Fig. 1a, Supplementary Fig. 1 and Extended Data Fig. 1) and this gave us confidence to use the Google mobility data as an estimate of general trends in emissions from surface transport. Correlations of the Apple driving data with Google transit data were stronger than 0.8 (during February–June 2020) for 37 countries and their trends typically agreed to within 20% for April 2020 (Extended Data Fig. 1). For the United Kingdom, Apple driving data agree well with government analysis of car journeys (Supplementary Fig. 2), whereas Google transit data appear to be more of a hybrid measure. Note, as discussed in the observational evidence section, NO_x emissions might be expected to be more closely aligned to commercial vehicles. Changes for these vehicles in the United Kingdom over the period of COVID-19 restrictions were less than indicated by either Apple or Google data (compare light van and heavy goods vehicle use to Google and Apple data in Supplementary Fig. 2). Therefore, we expect the Google mobility data to overestimate emission trends in the other sectors and we compare our approach for estimating granular near-real-time emission changes with the previous approaches of Liu et al.[2] and Le Quéré et al.[3] and with observations of NO_2 to test the assumptions.

The Le Quéré et al. sector analysis. Le Quéré et al.[3] analysed fossil fuel CO_2 emission changes in eight sectors (power, surface transport, residential, public and commercial, industry, national shipping, international shipping, national aviation and international aviation) and 69 countries representing 97% of global emissions. The Le Quéré et al. estimates are based on a global estimate of sector emission reductions according to a 1–3 level of confinement. The confinement level estimates were obtained from government (where accessible) and cross-media reports, while the sectoral activity data were from multiple streams of data for each sector including industry reports and were available daily or weekly. Changes in emissions as a function of the confinement level, for each sector, were estimated by quantifying changes in individual and industrial activity in each sector as a function of the observed level of confinement for all countries together. The data are then extrapolated for each country and each day, depending on their level of confinement and their mean emission levels in each sector. The United States and China were treated at state level and provincial level, respectively. Low, medium and high estimates of the emission changes resulting from uncertainty in the activity data among countries for different confinement levels were tested against our data. It was found that the high estimates agreed best with the Google transit trends during January to June 2020 (see Fig. 1 and Supplementary Figs. 1 and 2b). Projections for 2020 were also provided.

Mobility-based emission estimates. As mobility analysis does not cover all sectors or countries to make a global emission estimate we combine the mobility analysis with components of the analysis in Le Quéré et al.[3] to estimate global emission changes for CO_2 and other pollutants that were due to the COVID-19 restrictions.

We adopt the sector approach of Le Quéré et al.[3] but substitute their percentage changes in the emissions from surface transport, residential, public and commercial and industry sectors, with Google mobility changes in transit, residential, retail and recreation, and workplaces respectively. For the power sector, we used a hybrid approach, using a combined weighting of workplace, residential and retail mobility weighted by the 2019 national split of industrial, residential and commercial emissions. Then we used this weighted mobility measure to scale the power sector emissions. Finally, applying a scaling to match the global emission change in the power sector of the Le Quéré et al. high estimate. We also directly used the Le Quéré et al. emission trends for international and national aviation and shipping. In the 45 countries with only Google data available, the average emission changes from the 69 nations of Le Quéré et al. were used in the sectors not covered by the Google mobility data. Note that for simplicity and following Le Quéré et al., shipping changes are added to the surface-transport trends in the analyses presented in Fig. 2 and Supplementary Figs. 3 and 4. All emission changes are compared to a daily emission rate which is the annual averaged 2019 emission estimated for that country divided by 365 (using the data and approach from Le Quéré et al.). This assumption was tested by analysing the Liu et al.[2] data which included daily seasonal variation from 2019 and repeating our analysis on Climate Model Intercomparison Project Phase 6 (CMIP6) emission data[33] for NO_x as a test. We found that adding a seasonal cycle would decrease the January to May 2020 emission change estimate by 3%. However, as the Google analysis also does not account for a seasonal cycle, it is difficult to gauge the overall error in our estimates. To aid comparison with Le Quéré et al. and for consistency with the simple climate modelling approach discussed in Surface temperature change estimates, we choose not to introduce a seasonal cycle in our analyses. The combined dataset gives daily CO_2 emission changes for 2020, across eight sectors and 123 countries, covering 99% of global emissions. The high estimate of Le Quéré et al. and new mobility-based emission estimates were found to agree well with each other, both at the individual US state level and at the country level for the 56 countries with overlapping data (Supplementary Figs. 1, 3 and 4 and Fig. 1b).

Supplementary Table 1 compares the global average trends and that from some major nations to the CO_2 estimates in Le Quéré et al.[3] and that of Liu et al.[2]. Our trends are expected to be higher than the other datasets but this does not manifest itself for first-quarter trends in all countries. As the Google trends only start on 15 February, our analysis will underestimate first-quarter trend estimates where changes occurred before this date. More interesting are the differences with the Liu et al.[2] dataset for India and Russia, where their trends are considerably smaller. This could be caused by the differences with the reference assumptions. The approach of Liu et al.[2] makes a daily reference comparison with 2019 emissions and both nations show declining emissions in the first quarter of 2019, whereas our reference is taken as the Google mobility base-period of 3 January to 6 February (see The Google mobility analysis). As the emission data of Le Quéré et al.[3] are well-correlated in time with the Google mobility estimates and also quantitatively agree (see Supplementary Figs. 3 and 4), we assume that the mobility trends we see are largely a response to COVID-19. However, more work will be needed to fully understand and resolve these differences.

Non-CO_2 emission estimates. The Emission Database for Global Atmospheric Research (EDGAR) v.5.0 (ref. [14]) provides gridded and national-level sectoral emissions on methane, nitrous oxide and several short-lived species. The last year available is 2015. The sectors used in the EDGAR analyses are mapped onto the sectors from Le Quéré et al.[3] used here, according to the breakdown in Supplementary Table 2. The national- and sector-level emission changes for 2020 are then estimated by equation (1).

$$\Delta E_{\mathrm{in,is}}(t) = E\mathrm{base}_{\mathrm{in,is}}\frac{\Delta C_{\mathrm{in,is}}(t)}{C\mathrm{base}_{\mathrm{in,is}}} \quad (1)$$

where $\Delta E_{\mathrm{in,is}}(t)$ is the emission change (in kt day^{-1}) of the species as a function of nation (in) and sector (is). $E\mathrm{base}_{\mathrm{in,is}}$ is the annual emission divided by 365 of the species from the sector and nation for 2015. $\Delta C_{\mathrm{in,is}}(t)$ and $C\mathrm{base}_{\mathrm{in,is}}$ are the CO_2 emission change over 2020 and the average daily baseline emission, respectively, in the sector and nation being considered (CO_2 is in units of $MtCO_2$ day^{-1}). Similar equations are used for international aviation and shipping, where the global emission from aviation or shipping is ratioed by the globally averaged CO_2 emission change in the corresponding sum over the national change in sectors from the data of Le Quéré et al.[3]. The resulting changes are shown in Figs. 2 and 3 and Supplementary Figs. 5 and 6. Note that only fossil fuel CO_2 emissions were accounted for in Le Quéré et al., so the fractional changes refer to fossil fuel only. Agricultural and waste emissions are included in non-CO_2 analyses but assumed not to change. This leads to a reduced fraction of global emissions for non-CO_2 gases being covered and smaller emission changes for many species (Fig. 2). The assumption that a national sector's emission change will respond uniformly is obviously an important one. There are limited data to explore this assumption, although Liu et al.[2] and Le Quéré et al.[3] discuss how well it applies for CO_2 in specific sectors in specific countries. Extended Data Fig. 1 and Supplementary Fig. 2 and the discussion in CO_2 emissions estimates show that Google mobility data are unlikely to be a perfect proxy for NO_x trends in the United Kingdom but at least would be expected to be strongly correlated and close to the right magnitude. This is also supported by the NO_2 analysis in Fig. 3 and Supplementary Fig. 7. Our approach of assuming that national sectors change in the same way may partly explain why time series for CO_2 and non-CO_2 species evolve in a similar fashion in Fig. 2a. However, Supplementary Fig. 5 shows that sectors do evolve differently for different species. To examine this, we performed substitution tests where we crudely made large changes to specific national sector emissions time series or set them to zero. These tests suggested that the similar patterns seen across species in Fig. 2a are more a product of national restrictions evolving more-or-less together than of non-varying abatement choices within a national sector.

Emission scenarios. The generated datasets firstly combine sector-specific mobility changes referenced to the 3 January to 6 February 2020 period, with national lockdown measures. The method then uses published national emission inventories for either 2019 (for CO_2) or 2015 (for non-CO_2) to derive absolute emission changes which would also be relative to the early 2020 period. This reference is then projected out to 2030 to form an emission baseline representing current NDCs[15]. To explore the temperature response to emission changes relative to this baseline, the bottom-up emission change estimates from the first four months of 2020 have been extended according to the scenarios illustrated in Table 1. Four scenarios are explored: two-year blip, fossil-fuelled recovery, moderate green stimulus and strong green stimulus. The two-year blip scenario

assumes climate action to continue at the same level of ambition as implied by the current NDCs[15] until 2030—approximated by the implied global carbon price consistent with the emission reduction resulting from the NDCs. The fossil-fuelled recovery follows a path that lies 10% higher than the NDC path. The moderate green stimulus assumes about a 35% reduction in total global GHG emissions relative to the baseline NDC path and a further decline of global CO_2 emissions towards zero emissions in 2060. The Kyoto emissions totals of these NDC baskets are broken into components using the Silicone package[34] by interpolating between the MESSAGE-GLOBIOM implementations of the middle-of-the-road shared socioeconomic pathway (SSP2) scenarios[35,36]. Where CO_2 is defined directly, we interpolate from that instead. The strong green stimulus assumes about a 52% reduction in total global GHG emissions relative to the baseline NDC path and a further decline of global CO_2 emissions towards zero emissions in 2050. Non-CO_2 emissions are estimated by interpolating between the sustainability SSP1 scenarios implemented by the IMAGE model[37]. Scenarios are given as emissions of 39 species from anthropogenic and natural sources and volcanic and solar radiative forcing (see Smith et al.[21] for details). Only the ten species evaluated in this paper are changed. The original dataset gives annual emissions from 1750 to 2100 and these are linearly interpolated to monthly values, to provide higher time resolution for the subsequent calculations of effective radiative forcing and temperature.

Comparison to NO_2 observations. Hourly observations of NO_2 are taken from the OpenAQ database (https://openaq.org/) between 1 January 2018 and 3 May 2020, giving 1,747,189 hourly observations from 2,873 sites around the world. For each observation, a spatially and temporally co-located model value for the meteorological, chemical and emissions state is acquired from the NASA GEOS Composition Forecast (GEOS-CF) system. GEOS-CF integrates the GEOS-Chem chemistry model into the GEOS Earth System Model[38] providing global hourly analyses of atmospheric composition at $25\times25\,km^2$ spatial resolution in near-real-time. Anthropogenic NO_x emissions are prescribed using monthly HTAP bottom-up emissions[39], with annual scale factors based on OMI satellite data applied to it to account for year-over-year changes. GEOS-CF does not account for emission reductions related to COVID-19, providing a business-as-usual estimate of NO_2 that serves as a reference baseline for surface observations. For each site, a function describing the time-dependent model bias (observed value – modelled value) is developed using the 2018 and 2019 observations on the basis of the XGBoost algorithm[40], with the model meteorological, chemical and emissions states as the dependent variables. Of these data, 50% are used for training and 50% for testing. For 2020, we predict the concentration of NO_2, by taking the model output time series of NO_2 at each station and add the bias predicted by our trained algorithm. This then provides a counterfactual for the NO_2 concentration had COVID-19 restrictions not been put into place. We calculate the ratio between the actual concentration and that predicted for each site and then take the mean across all sites within a country. These data are compared to 26 country-level emission estimates in Supplementary Fig. 7 and the country-mean reductions compared to that predicted from the mobility data are shown in Fig. 2b.

Surface temperature change estimates. From the emission scenarios in Table 1, global averaged effective radiative forcing (ERF) and near-surface air temperature are computed. First, ERFs are calculated using the FaIR v.1.5 model and the methodology outlined in ref. [21] for 13 different forcing components. Uncertainties are estimated by 10,000 Monte Carlo samples of relative ERF uncertainties, using ranges based on IPCC Assessment Report 5 (ref. [41]), see ref. [21] for details. NO_x emissions affect direct forcing from nitrate aerosol and tropospheric ozone radiative forcing. Additionally, the ERF from aviation contrails and contrail-induced cirrus are assumed to scale with NO_x emissions from the aviation sector.

The two-layer energy balance model of Geoffroy et al.[42,43] including efficacy of deep ocean heat uptake is used to translate these ERF time series into surface temperature estimates. The five free parameters in this model are chosen to match individual CMIP6 model behaviour by fitting the parameters to $4\times CO_2$ abrupt simulations in 35 models; these parameter fits are shown in Supplementary Table 3. To estimate uncertainties, parameters corresponding to an individual model are picked randomly 10,000 times and paired to a sampled ERF parameter range for each of the 13 ERF time series. The two-layer model is then run with each of these parameter sets to make a surface temperature projection. The resulting plume of possible projections is then compared to Cowtan and Way[32] observed surface temperature record. The Cowtan and Way data have been adjusted to allow for the fact that the near-surface air temperature has warmed more than the sea surface temperature. To make this adjustment, the CMIP6 ratio of near-surface air temperature to blended near-surface air temperature and surface ocean temperatures is made over the historical period and found to converge towards 8% in recent years[44]. This is then used to scale the observations upwards. The root mean square errors of the simple model projections are then compared to these scaled observations over the period 1850–2019 inclusive. The goodness of fit is then used to provide projected probability distribution based on a weighted average of the goodness of fit. This follows the method outlined in Knutti et al.[45], with the exception that we do not downweight ensemble members on the basis of independence.

Testing the ozone forcing parameterization. The FaIR v.1.5 model used adopts a simple global annual mean emission-forcing relationship for tropospheric ozone which may not capture the seasonal and regional nuances of the atmospheric chemical response to the changes in NO_x and other emissions. To test this, a second ozone parameterization was used based upon source–receptor relationships from models that participated in the Task Force on Hemispheric Transport of Air Pollutants (TF-HTAP) project[46]. The parameterization[27,28] emulates the ozone response in models to applied perturbations in ozone precursor emissions (NO_x, CO and NMVOCs) and global CH_4 abundance. For emission perturbations in CO and NMVOCs a linear scaling factor is used whereas a nonlinear factor is used for changes in NO_x and CH_4. The 2020 annual mean tropospheric ozone radiative forcing and annual mean tropospheric ozone burden change deduced from this parameterization were $-0.029\,W\,m^{-2}$ and 7.5 Tg for the high emission scenario used here.

Data availability

A GitHub repository of the generated datasets is available from https://github.com/Priestley-Centre/COVID19_emissions and on Zenodo https://doi.org/10.5281/zenodo.3957826. Google LLC mobility data are available from https://www.google.com/covid19/mobility/ Apple LLC mobility data are available from https://www.apple.com/covid19/mobility EDGAR gridded emissions data are available from https://data.europa.eu/doi/10.2904/JRC_DATASET_EDGAR Cowtan and Way temperature observations are available from https://www-users.york.ac.uk/~kdc3/papers/coverage2013/had4_krig_annual_v2_0_0.txt Le Quéré et al.[3] emissions data are available from https://www.icos-cp.eu/gcp-covid19 The air quality data are available from https://openaq.org/. The GEOS modelled air pollution data used in this study/project have been provided by the Global Modelling and Assimilation Office at NASA Goddard Space Flight Center and are available from https://opendap.nccs.nasa.gov/dods/gmao/geos-cf/assim.

References

33. Hoesly, R. et al. Historical (1750–2014) anthropogenic emissions of reactive gases and aerosols from the Community Emissions Data System (CEDS). *Geosci. Model Dev.* **11**, 369–408 (2018).
34. Lamboll, R. D. et al. Silicone v1.0.0: an open-source Python package for inferring missing emissions data for climate change research (Geoscientific Model Development, 2020); https://doi.org/10.5194/gmd-2020-138
35. Rogelj, J. et al. Scenarios towards limiting global mean temperature increase below 1.5 °C. *Nat. Clim. Change* **8**, 325–332 (2018).
36. Fricko, O. et al. The marker quantification of the Shared Socioeconomic Pathway 2: a middle-of-the-road scenario for the 21st century. *Glob. Environ. Change* **42**, 251–267 (2017).
37. van Vuuren, D. P. et al. Energy, land-use and greenhouse gas emissions trajectories under a green growth paradigm. *Glob. Environ. Change* **42**, 237–250 (2017).
38. Hu, L. et al. Global simulation of tropospheric chemistry at 12.5 km resolution: performance and evaluation of the GEOS-Chem chemical module (v10-1) within the NASA GEOS Earth system model (GEOS-5 ESM). *Geosci. Model Dev.* **11**, 4603–4620 (2018).
39. Janssens-Maenhout, G. et al. HTAP_v2.2: a mosaic of regional and global emission grid maps for 2008 and 2010 to study hemispheric transport of air pollution. *Atmos. Chem. Phys.* **15**, 11411–11432 (2015).
40. Chen, T. & Guestrin, C. XGBoost: a scalable tree boosting system. Preprint at https://arxiv.org/abs/1603.02754 (2016).
41. Myhre, G. et al. in *Climate Change 2013: The Physical Science Basis* (eds Stocker, T. F. et al.) 659–740 (Cambridge Univ. Press, 2013). https://doi.org/10.1017/CBO9781107415324.018
42. Geoffroy, O. et al. Transient climate response in a two-layer energy-balance model. Part I: Analytical solution and parameter calibration using CMIP5 AOGCM experiments. *J. Clim.* **26**, 1841–1857 (2013).
43. Geoffroy, O. et al. Transient climate response in a two-layer energy-balance model. Part II: Representation of the efficacy of deep-ocean heat uptake and validation for CMIP5 AOGCMs. *J. Clim.* **26**, 1859–1876 (2013).
44. Richardson, M., Cowtan, K., Hawkins, E. & Stolpe, M. B. Reconciled climate response estimates from climate models and the energy budget of Earth. *Nat. Clim. Change* **6**, 931–935 (2016).
45. Knutti, R. et al. A climate model projection weighting scheme accounting for performance and interdependence. *Geophys. Res. Lett.* **44**, 1909–1918 (2017).
46. Koffi, B et al. *Hemispheric Transport of Air Pollution (HTAP) Specification of the HTAP2 Experiments: Ensuring Harmonized Modelling* (Publications Office of the European Union, 2016).

Acknowledgements

Funding was provided by the European Union's Horizon 2020 Research and Innovation Programme under grant nos. 820829 (CONSTRAIN) and UKRI NERC grant no. NE/N006038/1 (SMURPHS). C.D.J. was supported by the Joint UK BEIS/Defra Met Office Hadley Centre Climate Programme (GA01101) and CRESCENDO (EU Project 641816).

C.L.Q. was supported by the Royal Society grant no. RP\R1\191063 and the European Commission H2020 4C grant no. 821003. M.J.E. is grateful for computational support from the University of York's HPC service (Viking). We thank S. Forster for proofreading the paper and for useful ideas.

Author contributions

P.M.F. and H.I.F. designed the study. P.M.F. performed the main analyses with contributions from H.I.F. C.L.Q. provided the original data and contributed design ideas. C.J.S. provided the CMIP6 tuning of the two-layer model. C.K. and M.E. provided the surface NO_2 analyses. S.T. provided the ozone emulator analyses. M.G. and C.-F.S. contributed future scenario ideas. J.R. provided the scenario emission data with contributions from R.L. C.D.J. contributed the CO_2 concentration change discussion. D.R. contributed the wider air quality and societal context discussion. R.L. with initial work by T.R. provided the gridded online materials. All authors contributed to the writing.

Competing interests

The authors declare no competing interests.

Additional information

Extended data is available for this paper at https://doi.org/10.1038/s41558-020-0883-0.

Supplementary information is available for this paper at https://doi.org/10.1038/s41558-020-0883-0.

Correspondence and requests for materials should be addressed to P.M.F.

Reprints and permissions information is available at www.nature.com/reprints.

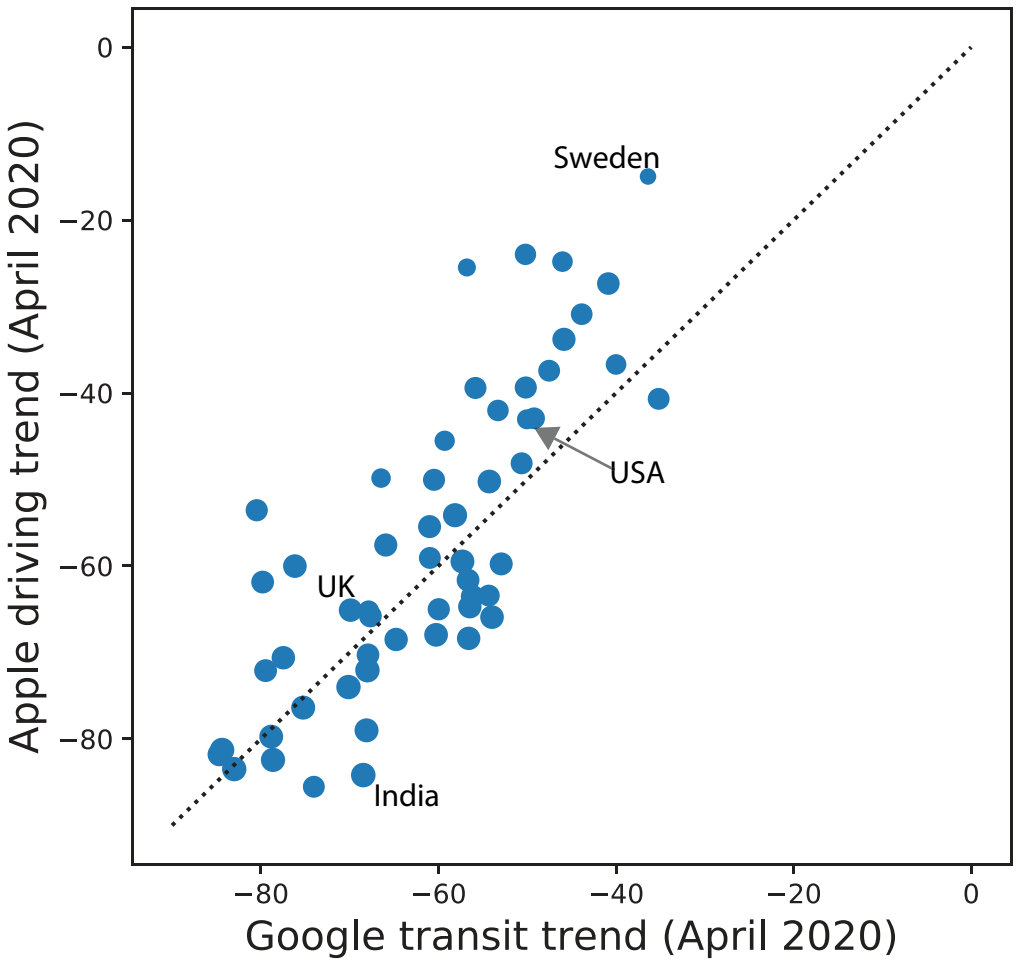

Extended Data Fig. 1 | Comparison of Google and Apple data. Comparison of Google and Apple data. The Apple driving change in April plotted against the Google transit change for available nations. Example countries are highlighted. The size of the symbol gives a measure of the correlation over Feb-June 2020, ranging from 0.39 for Sweden to over 0.96 (India). The dashed line indicates equality.

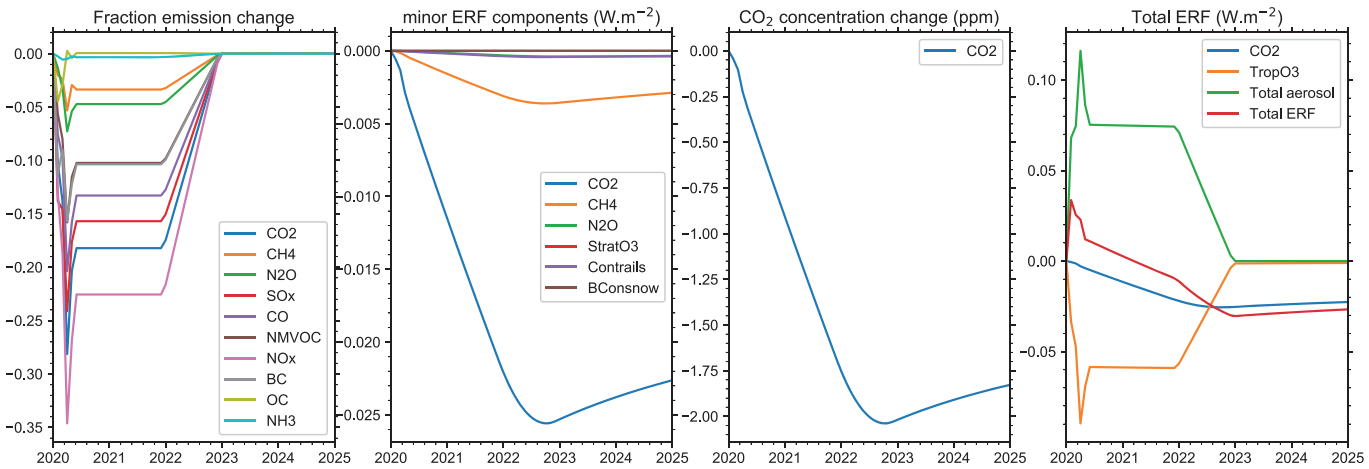

Extended Data Fig. 2 | Two-year blip scenario. Two-year blip scenario. Emissions, and best estimates of CO_2 concentration and effective radiative forcing (ERFs) components from the two-year blip scenario. Component ERFs are shown with minor ERFs in panel **b** and the three largest ERF changes in **c**.

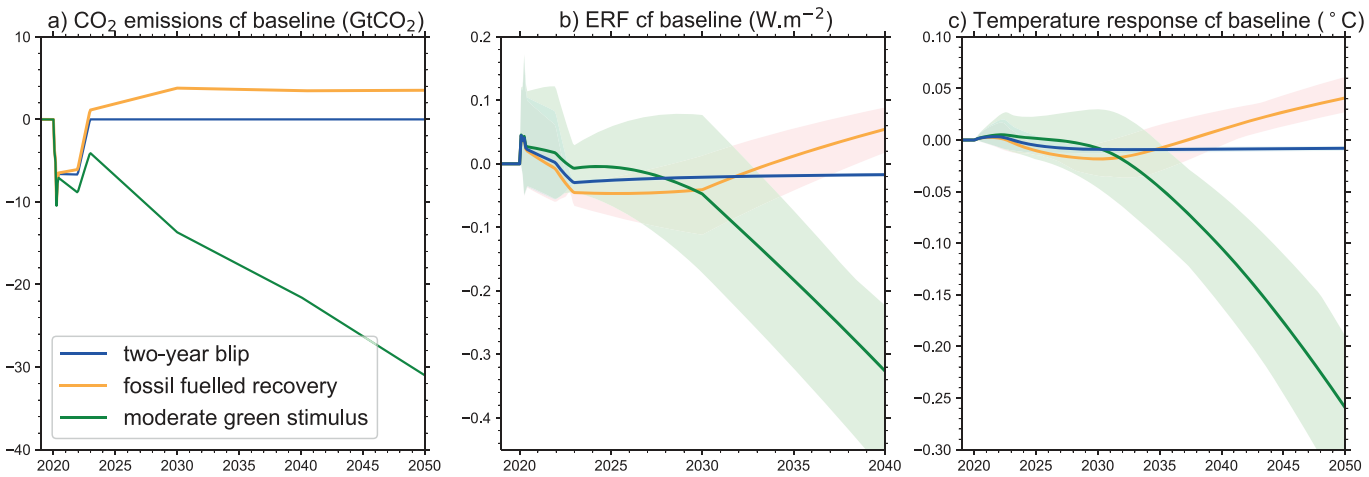

Extended Data Fig. 3 | Longer term climate projections to 2030. Longer term climate projections to 2030. Emissions, ERF and temperature response from the three scenarios over 2019-2030 (top). The probabilities are generated by varying the emulated CMIP6 model (one of 35) and ERF ranges with a 10,000 Monte Carlo sample. Distributions are weighted according to their goodness of fit over the historical period (see Methods surface temperature change estimates section).

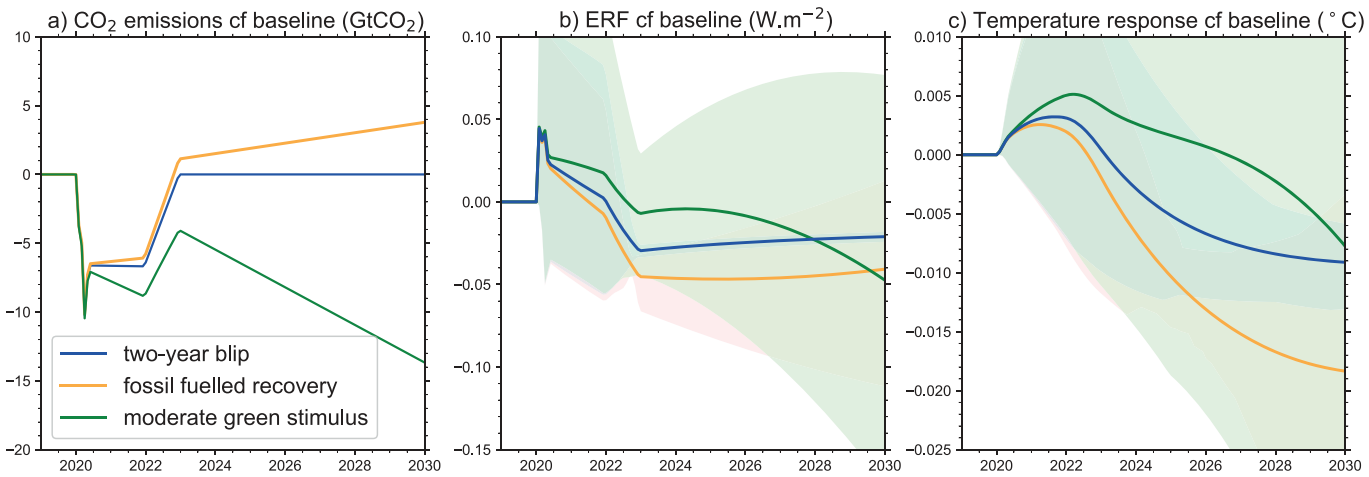

Extended Data Fig. 4 | Longer term climate projections to 2050. Longer term climate projections to 2050. As Extended Data Fig. 3 except for the period extended to 2019-2050.

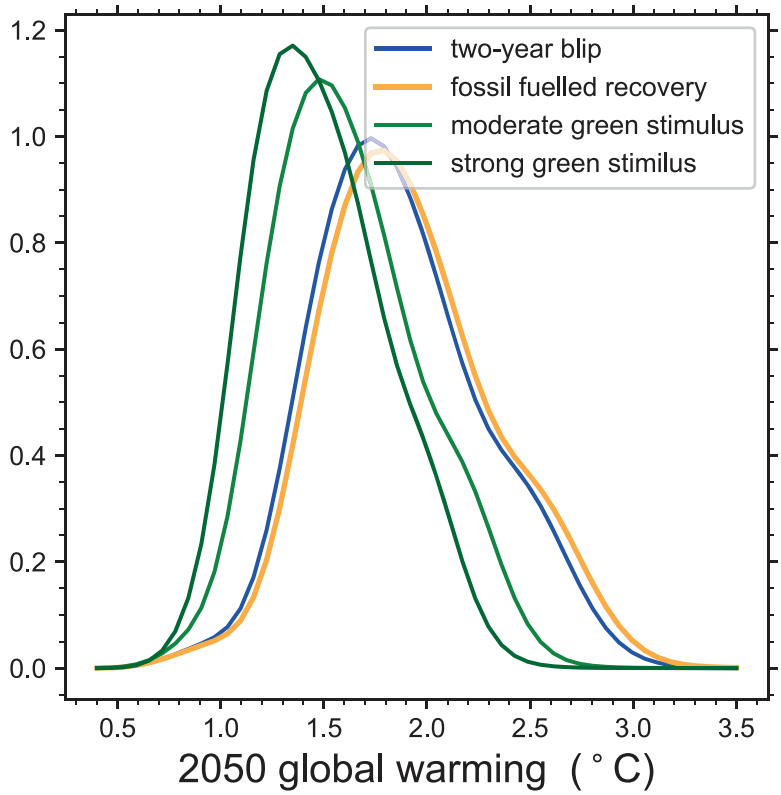

Extended Data Fig. 5 | Probability distributions of passing 2050 global warming levels. Probability distributions of passing 2050 global warming levels. Levels are relative to 1850-1900 for the scenarios in Table 1, generated by varying the emulated CMIP6 model (choosing one of 35 model formulations) and ERF ranges. Distributions are weighted according to their goodness of fit over the historical period (see Methods surface temperature change estimates section).